

miR-17-3p promotes the proliferation of multiple myeloma cells by downregulating P21 expression through LMLN inhibition

Pu Xiang¹ | Yiu To Yeung² | Jiheng Wang³ | Qiong Wu^{2,4} | Ruijuan Du^{2,4} |
 Chuntian Huang^{2,4} | Xuechao Jia^{2,4} | Yunfeng Gao² | Yafei Zhi^{2,4} |
 Fangqin Guo⁴ | Huifang Wei^{2,4} | Dandan Zhang² | Yuzhang Liu¹ | Lina Liu¹ |
 Lijie Liang¹ | Juan Wang¹ | Yongping Song¹ | Kangdong Liu^{2,4,5}  | Baijun Fang¹ 

¹Department of Hematology, Affiliated Cancer Hospital of Zhengzhou University and Henan Cancer Hospital, Henan Hematology Institute, Zhengzhou, Henan, China

²China-US (Henan) Hormel Cancer Institute, Zhengzhou, Henan, China

³Department of Head and Neck Thyroid, Affiliated Cancer Hospital of Zhengzhou University and Henan Cancer Hospital, Zhengzhou, Henan, China

⁴Department of Pathophysiology, School of Basic Medical Sciences, Zhengzhou University, Zhengzhou, Henan, China

⁵Cancer Chemoprevention International Collaboration Laboratory, Zhengzhou, Henan, China

Correspondence

Baijun Fang, Department of Hematology, Affiliated Cancer Hospital of Zhengzhou University and Henan Cancer Hospital, Henan Hematology Institute, Zhengzhou 450008, Henan, China.
 Email: bfang2018@163.com, zlyyfangbaijun1051@zzu.edu.cn

Kangdong Liu, Department of Pathophysiology, School of Basic Medical Sciences, Zhengzhou University; China-US (Henan) Hormel Cancer Institute; Cancer Chemoprevention International Collaboration Laboratory, Zhengzhou 450001, Henan, China.
 Email: kdliu@zzu.edu.cn

Funding information

National Natural Science Foundation of China, Grant/Award Number: 52110013; Zhongyuan Science and Technology Innovation Leadership Program, Grant/Award Number: 214200510023; Henan Innovation Talent Program, Grant/Award Number: 184200510007

Abstract

Multiple myeloma (MM), a hematological malignancy, has a poor prognosis and requires an invasive procedure. Reports have implicated miRNAs in the diagnosis, treatment and prognosis of hematological malignancies. In our study, we evaluated the expression profiles of miR-17-3p in plasma and bone marrow mononuclear cells of monoclonal gammopathy of undetermined significance (MGUS) and MM patients and healthy subjects. The results showed that the plasma and mononuclear cell expression levels of miR-17-3p in MM patients were higher than those in MGUS patients and normal controls. In addition, the expression of miR-17-3p was positively correlated with diagnostic indexes, such as marrow plasma cell abundance and serum M protein level, and positively correlated with the International Staging System stage of the disease. Receiver operating characteristic curve analysis suggested that miR-17-3p might be a diagnostic index of MM. Moreover, miR-17-3p regulated cell proliferation, apoptosis and the cell cycle through P21 in MM cell lines and promoted MM tumor growth in vivo. Furthermore, we predicted and verified LMLN as a functional downstream target gene of miR-17-3p. Negatively regulated by miR-17-3p, LMLN inhibits MM cell growth, exerting a tumor

Abbreviations: AUC, area under the curve; CCK-8, Cell counting kit-8; CRMM, complete remission MM; IHC, immunohistochemical; ISS, International Staging System; MGUS, monoclonal gammopathy of undetermined significance; MM, multiple myeloma; NC, negative control; NDMM, newly diagnosed MM; OD, optical density; ROC, receiver operating characteristic; RRMM, relapsed or refractory MM; WB, Western blotting.

Pu Xiang, Yiu To Yeung and Jiheng Wang contributed equally to this study.

This is an open access article under the terms of the Creative Commons Attribution-NonCommercial-NoDerivs License, which permits use and distribution in any medium, provided the original work is properly cited, the use is non-commercial and no modifications or adaptations are made.

© 2021 The Authors. *International Journal of Cancer* published by John Wiley & Sons Ltd on behalf of Union for International Cancer Control.

suppressive function through P21. Taken together, our data identify miR-17-3p as a promising diagnostic biomarker for MM in the clinic and unveil a new miR-17-3p-LMLN-P21 axis in MM progression.

KEYWORDS

LMLN, miR-17-3p, multiple myeloma, p21, plasma biomarker

1 | INTRODUCTION

Multiple myeloma (MM) is a complex hematologic malignancy characterized by abnormal clonal proliferation of plasma cells in the bone marrow (BM).¹ MM is the second most common blood disease, accounting for 12% of blood tumors in China.² The prognosis of MM is poor. The median survival time of patients treated with traditional chemotherapy is generally 3 years. Only 25% of patients survive for more than 5 years, and the median survival time for patients with advanced MM is only 6 months.³⁻⁵ Due to the consistently poor prognosis of MM, researchers are committed to defining the pathogenesis of MM and finding new treatment methods to improve its prognosis and survival rate.

In recent years, researchers have proven that miRNAs (endogenous small RNAs with a length of approximately 19-22 nucleotides⁶) play a role in the regulation of both gene expression and post-transcriptional modifications.⁷ miRNAs control the response, maturation, apoptosis and drug resistance of the immune cells,⁸⁻¹³ especially in the pathogenesis and prognosis of human tumors¹⁴ including solid tumors, such as bladder cancer,¹⁵ cervical cancer,¹⁶ breast cancer,¹⁷ as well as hematological tumors.¹⁸ In 2013, research findings suggested that miRNAs could be used for molecular diagnosis, thus improving the Mayo risk stratification of MM.¹⁹⁻²¹ In addition to being used as a diagnostic tool for MM, it was shown that miRNAs could be an important molecular marker for MM progression.²²⁻²⁷ The Mayo risk stratification system is based on the detection of abnormal genes, and it is an internationally recognized MM risk stratification method and prognosis indicator.^{28,29} The recurrence rate of MM is very high and is associated with serious complications that affect the overall survival of patients. To reduce the risk of recurrence and improve the survival of patients, Mayo risk stratification is recommended to assess the prognosis of patients and formulate corresponding treatment plans.³⁰ miR-17-92 clusters, such as miR-17, miR-18, miR-19a, miR-19b-1, miR-20, miR-32 and miR-92-1, are key miRNAs activated by Myc³¹ and are closely related to a high risk of MM.³²⁻³⁴ Previous studies have confirmed that miR-148a is highly expressed in MM, while CDKN1B is downregulated to promote the proliferation of myeloma cells.³⁵ However, the expression of miR-17-3p (a member of the miR-17-92 family) in MM cells is poorly characterized. In addition, data on the expression and role of plasma miR-17-3p in MM are scant. Therefore, our study investigated the expression of miR-17-3p in the plasma of MM patients and its correlation with clinical diagnostic indicators. We further explored miR-17-3p as a potential biomarker for the diagnosis of MM and explored its function and molecular mechanism.

What's new

MicroRNAs have shown potential in the diagnosis, treatment, and prognosis of hematological malignancies. Here, the authors found that miR-17-3p is highly expressed in the plasma and bone marrow cells of multiple myeloma patients. miR-17-3p expression is positively correlated with diagnostic indexes as well as the stage of disease. Moreover, miR-17-3p exerts an oncogenic role by regulating the proliferation, apoptosis, cell cycle, and colony formation of multiple myeloma cells by targeting LMLN and regulating P21. Altogether, the results identify miR-17-3p as a promising diagnostic biomarker and unveil the role of the miR-17-3p-LMLN-P21 axis in multiple myeloid progression.

2 | MATERIALS AND METHODS

2.1 | Patients and sample collection

Four newly diagnosed MM (NDMM) patients came from the Hematology Department of Henan Cancer Hospital in September 2015. These patients had experienced bone pain, anemia and renal damage, and the diagnosis was in accordance with the diagnostic criteria of the International Myeloma Working Group.³⁶ Four healthy subjects were included in the control group. Because of the small sample size, this cohort could not accurately reflect MM as a whole. Next, we expanded the sample size to verify these experimental results. All the participants (patients and controls) in our study gave written informed consent to be part of the study. The study protocol complied with the ethical guidelines of the Helsinki Declaration and was approved by the Scientific Ethics Committee of Henan Cancer Hospital. BM fluids were collected with anticoagulant EDTA-containing tubes (IDEXX Laboratories, Inc. USA). CD138+ cells in BM samples were enriched with whole blood sorting magnetic beads (Miltenyi Biotec, Germany). Trizol (Invitrogen, USA) extraction of total RNA was performed according to the manufacturer's instructions.

2.2 | Microarray analysis

The miRNA profile was determined and analyzed by GeneChip miRNA 4.0 Array (Affymetrix, USA) from the Affymetrix Microarray system (Affymetrix, USA).

Total RNA (1000 ng) was tailed by Poly(A) RNA polymerase, according to the manufacturer's protocol of the FlashTag Biotin HSR RNA Labeling Kit (Affymetrix, USA). RNA ligase was used to connect biotin-labeled signal molecules with the RNA, and the ligands and chips were hybridized using a GeneChip Hybridization Control Kit (Affymetrix, USA) at 60 rpm for 16 hours. After the chip hybridization, Fluidics Station 450 with AGCC Fluidics Control Software was used for washing and dyeing. Affymetrix Gene Chip Scanner 3000 scan chip results. The probe cell intensity files generated by the Affymetrix Gene Chip Command Console software were imported into probe-level summarization files for data extraction. The chip scanned images and raw data are generated in Expression Console Software and Transcriptome Analysis Console software by the AGCC operating system. Algorithm Options: One-Way Between-Subject ANOVA (unpaired). Default Filter Criteria: (a) Fold Change (linear) <-2 or Fold Change (linear) >2 ; (b) ANOVA *P*-value (Condition pair) $<.05$.

2.3 | Plasma and BM samples from MM patients

Plasma and BM samples were collected from same patients which included 10 monoclonal gammopathy of undetermined significance (MGUS) patients and 92 MM patients (Supplementary Table 1) in the Hematology Department of Henan Tumor Hospital from April 2013 to April 2018. The 10 MGUS patients included 6 males and 4 females. Out of the 92 MM patients, 38 were female and 54 were male. Among them, 22 had NDMM, 11 had complete remission MM (CRMM) and 59 had relapsed or refractory MM (RRMM). According to International Staging System (ISS) stage, there were 39 patients in ISS-I, 31 patients in ISS-II and 22 patients in ISS-III. The patients were between 24 and 85 years old, with an average age of 68 years. All MM patients met the diagnostic criteria of the 2011 National Comprehensive Cancer Network guidelines. We also recruited 20 (7 women and 13 men) healthy volunteers as a control group. All patients and healthy subjects recruited in the study provided written informed consent. The study protocol conformed to the ethical guidelines of the Helsinki Declaration and was approved by the Scientific Ethics Committee of Henan Cancer Hospital.

2.4 | Collection of plasma samples

Venous blood was collected with an anticoagulant EDTA-containing tube. The samples were centrifuged at 1200g for 15 minutes at 4°C, and the supernatant was transferred into a clean 1.5 mL centrifuge tube. The supernatant was further centrifuged at 12000g for 10 minutes at 4°C. The supernatant was carefully transferred to new 1.5-mL enzyme-free centrifuge tubes. The plasma samples were stored in a -80°C refrigerator until needed for experiments.

2.5 | Collection of BM mononuclear cells

BM fluids from MGUS patients, MM patients and healthy subjects were extracted and treated with lymphocyte separation medium

(Sigma, USA), according to the manufacturer's protocol. Finally, the white membrane was absorbed and washed in 1× PBS, and then the samples were centrifuged. The BM mononuclear cells were collected as a precipitate.

2.6 | BM smear

BM aspirate smears had been prepared from the first pull samples. Slides had been stained by Giemsa and the proportion of BM plasma cells (BMPCs) had been quantified by counting 500 nucleated cells. In case of significant dilution with peripheral blood ($<15\%$ myeloid precursor cells and erythroid), smears had been classified as not qualified.

2.7 | Cell culture

The human MM cell lines U266B1 (RRID: CVCL_0566), KMS-11 (RRID: CVCL_2989) and MM1.R (RRID: CVCL_8794) were donated by Beijing Shadong Biotechnology Co, Ltd. NCI-H929 (RRID: CVCL_1600) and RPMI-8226 (RRID: CVCL_0014) cells were purchased from Nanjing Kebai Biological Co, Ltd, while Lenti-X 293T (RRID: CVCL_0063) cells were donated by the China-US (Henan) Hormel Cancer Institute. All human cell lines have been authenticated using STR profiling (Genomic DNA was extracted from the provided cells and compared with the information in ATCC, DSMZ, jcrb and RIKEN databases to detect whether there was cross contamination in the cells.) within the last 3 years. All experiments were performed with mycoplasma-free cells. The KMS-11 cells were maintained in Iscove's modified Dulbecco's medium (Gibco, USA) supplemented with 10% fetal bovine serum (FBS) (Thermo Fisher Scientific, USA). MM-1R, RPMI-8226 and NCI-H929 cells were maintained in RPMI-1640 medium. MM-1R and RPMI-8226 cells were supplemented with 10% FBS, while NCI-H929 cells were supplemented with 0.05 mM β -mercaptoethanol. Lenti-X 293T cells were cultured in Dulbecco's minimum essential medium (Gibco, USA) with 10% FBS. The cells were incubated at 37°C in a humidified atmosphere with 5% CO_2 .

2.8 | RNA isolation and RT-PCR

Total RNA was extracted from plasma using TRIzol LS Reagent (Invitrogen, USA), while total RNA from both the BM mononuclear cells and MM cell lines was extracted using TRIzol reagent (Invitrogen, USA) according to the manufacturer's protocol. The concentration of extracted RNA was approximated by a NanoDrop 2000 spectrophotometer (Thermo Fisher Scientific, USA). Complementary DNA (cDNA) was synthesized from miRNA using a Prime Script RT reagent kit (Takara, Japan). Relative quantitative RT-PCR was performed by SYBR Premix Ex Taq II kit (Takara, Japan) on a PRISM 7900HT system (Thermo Fisher Scientific, USA). Our study targeted the hsa-miR-17-3p gene using U6 as the internal reference gene, and LMLN gene

using β -actin as the reference gene. The experiments were carried out in triplicate, and the results were analyzed by the $2^{(-\Delta\Delta CT)}$ method. The primer sequences for reverse transcription and RT-PCR are shown in Supplementary Table 2.

2.9 | Receiver operating characteristic (ROC) curve analysis

ROC curves were used to illustrate the response of the subjects to the signal stimulation. The graphical plots were made according to the response result, taking the sensitivity (true positive rate) as the ordinate and 1-specificity, that is, the false positive rate, as the abscissa. The area under the curve (AUC) determined the accuracy of an index. The point closest to the top left corner of the coordinate graph represents the critical value having the highest sensitivity and specificity of the studied index. IBM SPSS 22.0 software was used to generate the ROC curves. The expression levels of plasma miR-17-3p in the 22 NDMM patients and 20 healthy subjects were expressed as ΔCT ($\Delta CT = \text{average CT}_{(\text{miR-17-3p})} - \text{average CT}_{(\text{U6})}$).

2.10 | Correlation analysis

Correlation analysis refers to the statistical analysis of two or more variables to determine whether they are correlated and to determine the degree of correlation. Since the ratio of BMPCs and the content of M protein are important indicators for the diagnosis of MM, correlation analysis was conducted to understand whether the expression of plasma miR-17-3p was correlated with the above indicators. The correlation experiment could help understand whether plasma miR-17-3p has the potential to be a biomarker for the diagnosis of MM. While GraphPad Prism 6.0 software was used to perform the correlation analyses, the expression level of plasma miR-17-3p in the 22 NDMM patients was expressed as ΔCT ($\Delta CT = \text{average CT}_{(\text{miR-17-3p})} - \text{average CT}_{(\text{U6})}$).

2.11 | Lentiviral construction and infection

The PLKO.1 plasmid was a kind donation from the China-US (Henan) Hormel Cancer Institute. The shLMLN was constructed according to the manufacturer's protocol. The primer sequences for shRNA were shLMLN-1-F: 5'-CCGGC CACAGTGAACATGAGGTTACTCGAGTACCTCATGTTTCACTGTGGTTTTG-3'; shLMLN-1-R: 5'-AATCAA AAACCACAGTGAACATGAGGTTACT CGAGTAACCTCATGTTTCAC TGTGG-3'; shLMLN-2-F: 5'-CCGGCAGA CTTT GTTCTTTACG TTCTCGAGAACGTAAAGAAACAAGTCTGCTTTTTG-3'; and shLMLN-2-R: 5'-AATCAAAAAGCAGACTTTGTTCTTTACGTTCTCGAGA ACGTA AAGAACAAGTCTGC-3'. The miR-17-3p-LV3 (miR-17-3p over-expressed plasmids), SJNC (control vector) and miR-17-3p-inhibitor plasmids were purchased from Gene Pharma, and the LMLN over-expression plasmid was purchased from You Bio. Three plasmid packaging systems (PSPAX₂, PMD₂G and target plasmid) were used to package

lentivirus in Lenti-X 293T cells, and the volume ratio of transfection reagent Simple-fect (Thermo Fisher Scientific, USA) to total plasmid mass was 2:1.

Cells were cultured with lentivirus and 8 $\mu\text{g}/\text{mL}$ polybrene for 24 hours. Puromycin was then used to screen and select cells that stably expressed the virus. The transduction efficiency was detected by both RT-PCR and Western blot (WB) experiments.

2.12 | Transient transfection

miR-17-3p-mimics, negative control (NC), miR-17-3p-inhibitor and inhibitor-NC were purchased from Gene Pharma. The transfection reagent Lipo2000 (Thermo Fisher Scientific, USA) was used in the experiments, according to the manufacturer's protocol.

2.13 | Cell counting kit-8 (CCK-8) assay

Cells were spread in a 96-well plate (1.5×10^4 cells per well) containing 200 μL of the medium and grown overnight in a 37°C incubator containing 5% CO₂. Then, 20 μL of CCK-8 reagent was added to the cells and incubated for 4 hours at 37°C in an incubator containing 5% CO₂. Optical density (OD) values were measured at intervals of 0, 24, 48, 72 and 96 hours.

2.14 | Colony formation in soft agar

Three milliliters of soft agar were added to six wells of a plate, and the samples were incubated at room temperature for 30 minutes. One milliliter of media containing 8000 cells was added on top of the agar and incubated for 1 week at 37°C in an incubator containing 5% CO₂. The growth and size of colonies were observed under a microscope once a day. After the colonies grew to a certain extent, each well of the plate was randomly imaged 3 to 5 times.

2.15 | Invasion and migration assays

Invasion assay was conducted in transwell chambers (Costar, Corning Inc, USA) inserted in the 24-well plates. 2.0×10^5 cells were suspended in 100 μL serum-free medium in the upper side of Matrigel-coated transwell chamber, and 500 μL medium with 10% FBS in the basolateral chamber, and incubated for 48 hours in a 37°C incubator containing 5% CO₂. Migration assay was conducted in the same procedures except for Matrigel precoating. Because the MM cell lines are suspended cells, the cells which invaded or migrated through the membrane are suspended in the culture medium of basolateral chamber, and these cells cannot be fixed and stained. Alternatively, we counted the invaded or migrated cells by cell counter (Thermo Fisher Scientific, USA). After 48 hours

incubation, the chambers were taken out and the basolateral chamber membrane and lower chamber were washed by $1 \times$ PBS for three times. Finally, all the liquid was collected into 1.5 mL centrifuge tube. Then, we centrifuge the liquid containing collected cells and discard the supernatant, resuspend the cells with 200 μ L medium, take appropriate amount of cell suspension and count with the cell counter. Each group had three multiple wells, and the invasion and migration experiments had three independent biological replicates, respectively.

2.16 | Cell cycle assay

Triplicates of 5×10^5 cells per group per well were seeded in a six well plate, and 2 mL of medium was added. The cells were cultured at 37°C for 48 hours in an incubator containing 5% CO_2 . The cells were collected and washed in $1 \times$ PBS. The cells were fixed with ice anhydrous ethanol for at least 2 hours. Five microliters of RNase (10 mg/mL) was added to each tube and incubated for 1 hour at room temperature. Then, 5 μ L PI (10 mg/mL) was added to each tube and incubated in the dark at room temperature for 15 to 20 minutes. We then added 100 to 300 μ L (depending on the number of cells) of 0.6% Triton $\times 100$ and mixed the samples. The cell suspension was transferred into the flow cytometer (Thermo Fisher Scientific, USA) for cell cycle analysis.

2.17 | Apoptosis experiment

Triplicates of 5×10^5 cells per group were seeded per well in a six well plate, and 2 mL of medium was added. The cells were cultured at 37°C for 48 hours in an incubator containing 5% CO_2 . The cells were collected and washed in $1 \times$ PBS, and then the supernatant was discarded after centrifugation. Annexin V binding buffer was used to suspend the cells at a concentration of $0.25\text{--}1.0 \times 10^7/\text{mL}$. After transfer of 100 μ L of cell suspension into the flow tube, 5 μ L of APC-Annexin V was added to each tube. Five microlitres of 7-AAD viability staining solution was added to each tube and then gently mixed before incubation at room temperature in the dark for 15 minutes. After the addition of 300 μ L of Annexin V Binding Buffer to each tube, cell apoptosis was measured by flow cytometry (Thermo Fisher Scientific, USA).

2.18 | Western blotting (WB)

The collected cell precipitate was lysed with RIPA lysis buffer, and the protein concentration was measured using a bicinchoninic acid kit (Sigma, USA) according to the manufacturer's protocol. The protein samples were run on SDS-PAGE gels and transferred to PVDF membranes. The samples were blocked in 5% skimmed milk at room temperature for 1 hour. Afterward, LMLN primary antibody (#HPA028844, Sigma, USA) or P21 primary antibody

(#2947, CST, USA) was incubated overnight at 4°C , and then the membrane was washed three times in $1 \times$ TBST. Goat anti-Rabbit IgG (#6990, CST, USA) was added and incubated on a shaker at room temperature for 1 hour. The samples were washed three times in $1 \times$ TBST. The ECL luminescent chromogenic solution was used to develop the blot before observation under a chemiluminescence imaging system (Bio-Rad, USA).

2.19 | Construction of dual-luciferase vector and assays

The target hsa-miR-17-3p genes were predicted by miRBase, miRDB, TargetScan and miRWalk and verified by both RT-PCR and WB. mRNAs whose expression levels were inversely correlated with those of miR-17-3p were considered possible target genes. Approximately 400 bp of the 3'-UTR segment of the possible target gene, including the binding site, was incorporated into the pmirGLO vector (Promega, USA) to construct a recombinant plasmid according to the manufacturer's protocol. Then, the recombinant plasmid was transfected into HEK293T cells with miR-17-3p mimics and NC, inhibitors and inhibitor-NC. The cells were incubated for 48 hours after transfection. The dual-luciferase vector reporting experiment was detected and analyzed by the Dual-Luciferase Reporter Assay System (Promega, USA), and the experiment was repeated after the predicted binding site was mutated. The wild-type and mutant sequences of the binding site are shown in Figure 6A. The upstream and downstream primer sequences for PCR are shown in Supplementary Table 3, and the primer sequences of the recombinant plasmid are shown in Supplementary Table 4.

2.20 | Rescue experiment

NCI-H929 cells were placed in three 6-cm dishes at a density of 5×10^5 cells/well. The cells were infected with lentiviruses, and polybrene (8 $\mu\text{g}/\text{mL}$) was added for 24 hours. CCK-8, RT-PCR and WB assays were then performed to evaluate differences between the groups.

2.21 | Xenograft experiment

A total of 18 female Nu/Nu mice, aged 6 to 8 weeks, were used in the experiment. Briefly, the mice were divided into two groups: 9 in the miR-17-3p overexpression group and 9 in the miR-17-3p knockdown group. The test animals were carefully selected to ensure no significant differences in their weight. The mice were fed in the animal center at Zhengzhou University laboratory. Cages, water, food and other objects in contact with the mice were autoclaved for sterilization. The mice eat and move freely in the cages.

Packaging and targeting plasmids were transfected into Lenti-X 293T cells using the Simplefect transfection reagent, and 8 $\mu\text{g}/\text{mL}$

polybrene was used to infect NCI-H929 cells for 24 hours. Infected cells were selected by RPMI 1640 medium containing 8 $\mu\text{g}/\text{mL}$ puromycin. When the cells had grown enough, each nude mouse was subcutaneously injected with 100 μL of PBS suspension containing 1×10^7 cells. One week later, mouse skin was monitored for the occurrence and growth of tumors, and then the tumor sizes and weights were recorded every 3 days. The average tumor weight did not exceed 2 g. The study protocol conformed to the ethical guidelines of the Helsinki Declaration and was approved by the Scientific Ethics Committee of Henan Cancer Hospital.

2.22 | Immunohistochemistry

Paraffin-embedded sections (5- μm thick) were prepared for immunohistochemical (IHC) analysis. After deprotection of the antigen, the sections were blocked with 5% goat serum, incubated overnight at 4°C and Ki-67 detected using an antibody (#PA519462, Thermo Fisher Scientific, USA). After incubation with rabbit secondary antibody, protein targets were visualized by 3,3'-diaminobenzidine staining according to the manufacturer's instructions. The sections were counterstained with hematoxylin and dehydrated with xylene under a series of different grades of alcohol. They were then placed onto glass slides under glass cover slips and observed using a microscope.

3 | STATISTICAL ANALYSIS

Data obtained were analyzed using GraphPad Prism 6.0 software. Continuous variables were presented as mean \pm SD. Noncategorical variables were compared by *t* test. Correlation between plasma miR-

17-3p expression and BMPCs or the content of serum M protein in NDMM patients was analyzed by Pearson correlation analysis. ROC curves were performed to evaluate the diagnosis value of plasma miR-17-3p in NDMM patients. *P* value $<.05$ was considered to be statistical significance.

4 | RESULTS

4.1 | miR-17-3p is highly expressed in the BM of MM patients

To determine the role of miRNAs in the development of MM, we used a miRNA 4.0 microarray to detect miRNAs with abnormal expression and further study their function. The results indicated that there were 161 miRNAs with abnormal expression. Compared to the normal subjects, in the NDMM patients, 38 miRNAs had lower expression and 123 miRNAs had higher expression (Figure 1A). To verify whether the differentially expressed miRNAs in miRNA 4.0 Chip were consistent with those in BM mononuclear cells of the discovery cohort, we also extracted and detected the expression of the first nine miRNAs in BM mononuclear cells from four patients and four healthy samples. Although the expression of miRNAs varied greatly among individuals, the trend of the results was consistent with those of miRNA 4.0 Chip (Figure 1B). However, the results showed that the expression of miR-17-3p in NDMM patients was stable, while the top three miRNAs were significantly different. We think that miR-17-3p was more suitable as a tumor marker and may play an important role in MM development. Therefore, we chose miR-17-3p for further study. To further confirm our speculation, we collected samples from 10 MGUS patients, 92 MM patients (22 NDMM, 11 CRMM and 59 RRMM; according to ISS stage, there were 39 patients in ISS-I, 31 patients in

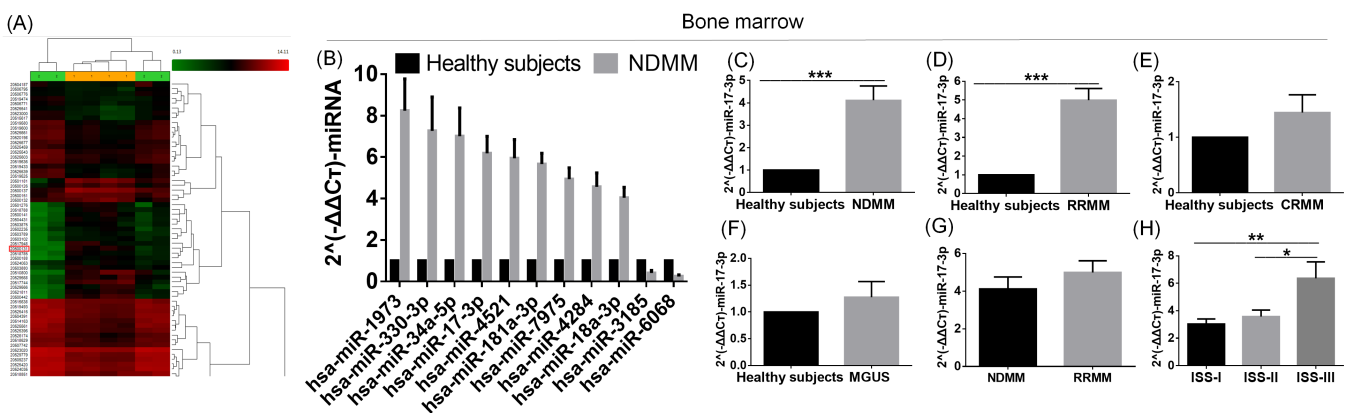


FIGURE 1 Expression of miR-17-3p in the bone marrow of multiple myeloma (MM) patients. A, miRNA 4.0 microarray showed that miR-17-3p is more highly expressed in the bone marrow of newly diagnosed MM (NDMM) patients than in that of healthy subjects. Number 1 on the orange background represents the NDMM patient and the number 2 on the green background represents the healthy subjects. B, Expression of the first nine upregulated miRNAs and two downregulated miRNAs in NDMM patients from the bone marrow mononuclear cells from four patients and four healthy samples. C-F, Expression of miR-17-3p in the bone marrow of healthy subjects and NDMM patients (C), RRMM patients (D), CRMM patients (E), and MGUS patients (F). G, Expression of miR-17-3p in the bone marrow of NDMM and RRMM patients. H, RT-PCR analysis of miR-17-3p expression in Grade I ($n = 39$), Grade II ($n = 31$) and Grade III ($n = 22$) MM patients. U6 was the internal reference. The results were analyzed by the $2^{(-\Delta\Delta\text{CT})}$ method ($*P < .05$; $**P < .01$; $***P < .001$) [Color figure can be viewed at wileyonlinelibrary.com]

ISS-II and 22 patients in ISS-III) and 20 healthy subjects to detect the expression level of miR-17-3p in BM. The findings showed that the expression levels of miR-17-3p in the NDMM patients and RRMM patients were higher than those in the healthy subjects (Figure 1C,D; $***P < .001$). Although the expression of miR-17-3p in the CRMM and MGUS patients was higher than that in the healthy subjects and the expression of miR-17-3p in the RRMM patients was higher than that in the NDMM patients, the results were not statistically significant (Figure 1E-G; $P > .05$). In addition, we found that the expression of miR-17-3p was positively correlated with ISS stage (Figure 1H).

4.2 | miR-17-3p is highly expressed in the plasma of MM patients

Since the expression of miR-17-3p was high in the BM of MM patients, whether miR-17-3p can be used as a plasma biomarker for the diagnosis of MM was investigated. We collected samples from 10 MGUS patients, 92 MM patients and 20 healthy subjects to analyze the expression of miR-17-3p in plasma. The results showed that the expression levels of plasma miR-17-3p in the NDMM and RRMM patients were higher than those in the normal controls (Figure 2A,B; $***P < .001$; $**P < .01$). Although the expression of plasma miR-17-3p in the CRMM and MGUS patients was higher than that in the healthy subjects and the expression of miR-17-3p in the RRMM was higher than that in the NDMM, the results were not statistically significant (Figure 2C-E; $P > .05$). In conclusion, the results showed that the BM and plasma expression of miR-17-3p in the MM patients was higher than that in the MGUS patients and healthy subjects. In addition, the expression of plasma miR-17-3p was positively correlated with ISS stage (Figure 2F). In summary, the expression of miR-17-3p in plasma was consistent with that in BM.

We further explored the correlation among plasma miR-17-3p expression, BMPC abundance and serum M protein expression in NDMM patients. The results showed that plasma miR-17-3p expression in NDMM patients was closely associated with the abundance of BMPCs (Figure 2G; $P < .01$, $r = .625$) and the level of serum M protein (Figure 2H; $P < .05$, $r = .429$). This result suggested that plasma miR-17-3p may be a molecular marker for the diagnosis of MM. We then used the ROC curve to determine the accuracy of plasma miR-17-3p as a molecular marker for the diagnosis of MM. The ROC curve of plasma miR-17-3p expression in normal controls and NDMM patients had an AUC of 0.755. (Figure 2I; $P = .005$). These data suggested that plasma miR-17-3p has high specificity and sensitivity as a biomarker for the diagnosis of MM.

4.3 | miR-17-3p is an oncogene in MM cell lines

We previously showed that miR-17-3p is highly expressed in the BM and plasma of MM patients. Lijuan Chen et al have found that miR-17 could promote MM cell proliferation, and both miR-17-3p and miR-17-5p are codified by the miR-17-HG. Our previous microarray

analysis showed that miR-17-3p was highly expressed in NDMM BM, but miR-17-5p was not detected. Therefore, we believe that miR-17-3p and miR-17-5p may not play the same role in MM, and miR-17-3p was more valuable for research. We then used RT-PCR to detect the expression of miR-17-3p in five MM cell lines and normal human BM mononuclear cells. The results suggested that miR-17-3p is more highly expressed in MM cell lines than in normal human BM mononuclear cells (Figure 3A). To further investigate whether miR-17-3p affects MM cell proliferation, we transfected NCI-H929 and RPMI-8226 cells with miR-17-3p mimics and transfected NCI-H929 and KMS-11 cells with miR-17-3p inhibitors; then, we used RT-PCR to measure miR-17-3p expression levels. Our results showed that transfection of miR-17-3p mimics increased miR-17-3p expression and transfection with inhibitors decreased its expression in the transfected cells compared to the control cells (Figure 3B; $**P < .01$). Next, we conducted a CCK-8 assay to assess whether miR-17-3p promotes cell proliferation. The results showed that overexpression of miR-17-3p promoted cell proliferation, while miR-17-3p knockdown inhibited cell proliferation (Figure 3C; $*P < .05$; $**P < .01$). Then, we studied the effect of miR-17-3p on cell colony formation by soft agar assay. The findings showed that miR-17-3p overexpression promoted cell colony formation, while miR-17-3p knockdown inhibited cell colony formation compared to that in the control group (Figure 3D; $*P < .05$; $***P < .001$).

Since we showed that miR-17-3p could promote cell proliferation, we wanted to further check its effect on cell apoptosis and the cell cycle. We found that miR-17-3p inhibited apoptosis (Figure 3E; $*P < .05$) and affected the cell cycle of MM cells (Figure 3F; $*P < .05$; $**P < .01$). The results showed that after overexpression of miR-17-3p, the proportion of G1 + S phase cells increased, while the proportion of G2 phase cells decreased compared to that in the control; conversely, when miR-17-3p expression was suppressed, the proportion of G1 + S phase cells decreased, and the proportion of G2 phase cells increased. To clarify the mechanism by which miR-17-3p affects the cell cycle of MM cells, we identified the related cyclin and cyclin-dependent kinase (CDK) inhibitor by WB. The results showed that the expression of P21 protein was negatively correlated with the expression of miR-17-3p (Figure 3G,H). Therefore, we believe that miR-17-3p can affect the expression of P21 through some mechanism and then affect the cell cycle and proliferation.

4.4 | LMLN is a target gene of miR-17-3p and is negatively regulated by miR-17-3p

To explore the mechanism by which miR-17-3p regulates MM cell proliferation, apoptosis and the cell cycle, we used bioinformatics methods to search for potential downstream target genes regulated by miR-17-3p. There were 500 genes that were predicted by three software programs (Figure 4A), and we screened 11 genes related to cell proliferation, colony formation, apoptosis and the cell cycle. Because miR-17-3p was moderately expressed in NCI-H929 cell line, we transfected NCI-H929 cells with miR-17-3p mimics or inhibitor and used RT-PCR to measure the 11 genes expression levels. RT-PCR

results showed that LMLN is negatively regulated by miR-17-3p (Figure 4B). LMLN is a leishmanolysin-like peptidase and could encode a zinc-metallopeptidase, which may play a role in cell migration,

invasion and mitotic progression.³⁷ At present, there are few studies on this gene in MM. To further verify this result, we transfected NCI-H929 and RPMI-8226 cells with miR-17-3p mimics and transfected

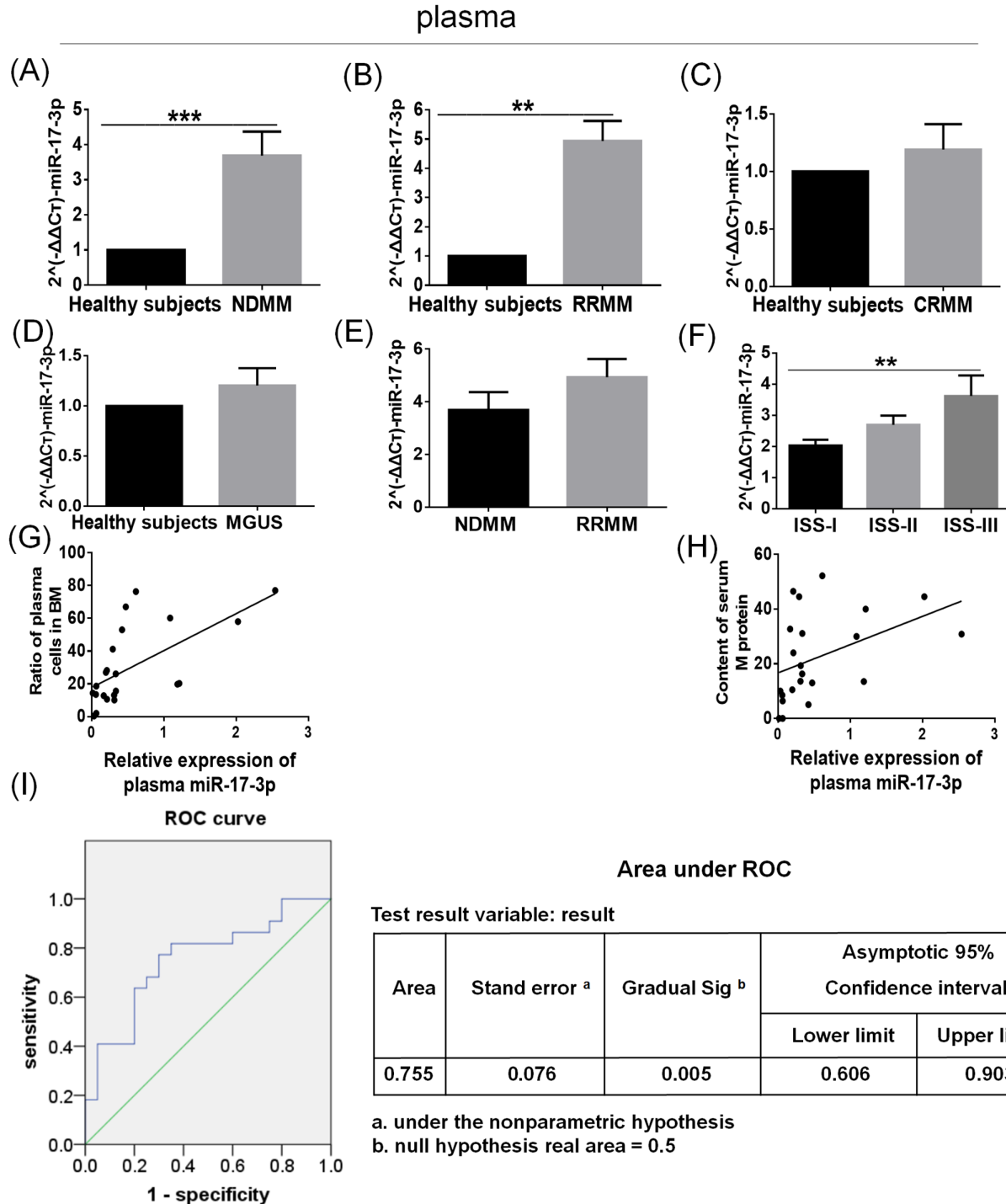


FIGURE 2 miR-17-3p is highly expressed in the plasma of multiple myeloma (MM) patients and has clinical diagnostic value. A-D, Expression levels of plasma miR-17-3p in healthy subjects and 22 NDMM (A), 59 RRMM (B) and 11 CRMM (C) and 10 MGUS patients (D). E, Expression levels of plasma miR-17-3p in NDMM and RRMM patients. F, RT-PCR analysis of plasma miR-17-3p expression in Grade I (n = 39), Grade II (n = 31) and Grade III (n = 22) MM patients. G, In newly diagnosed MM (NDMM) patients, plasma miR-17-3p and the abundance of bone marrow plasma cells were positively correlated ($r = 0.625$, $P = .002$); H, plasma miR-17-3p and serum M protein were also positively correlated ($r = 0.429$, $P = .046$). I, Receiver operating characteristic (ROC) curve of plasma miR-17-3p expression in NDMM patients and healthy subjects. The AUC was 0.755, $P = .005$ (** $P < .01$, *** $P < .001$) [Color figure can be viewed at wileyonlinelibrary.com]

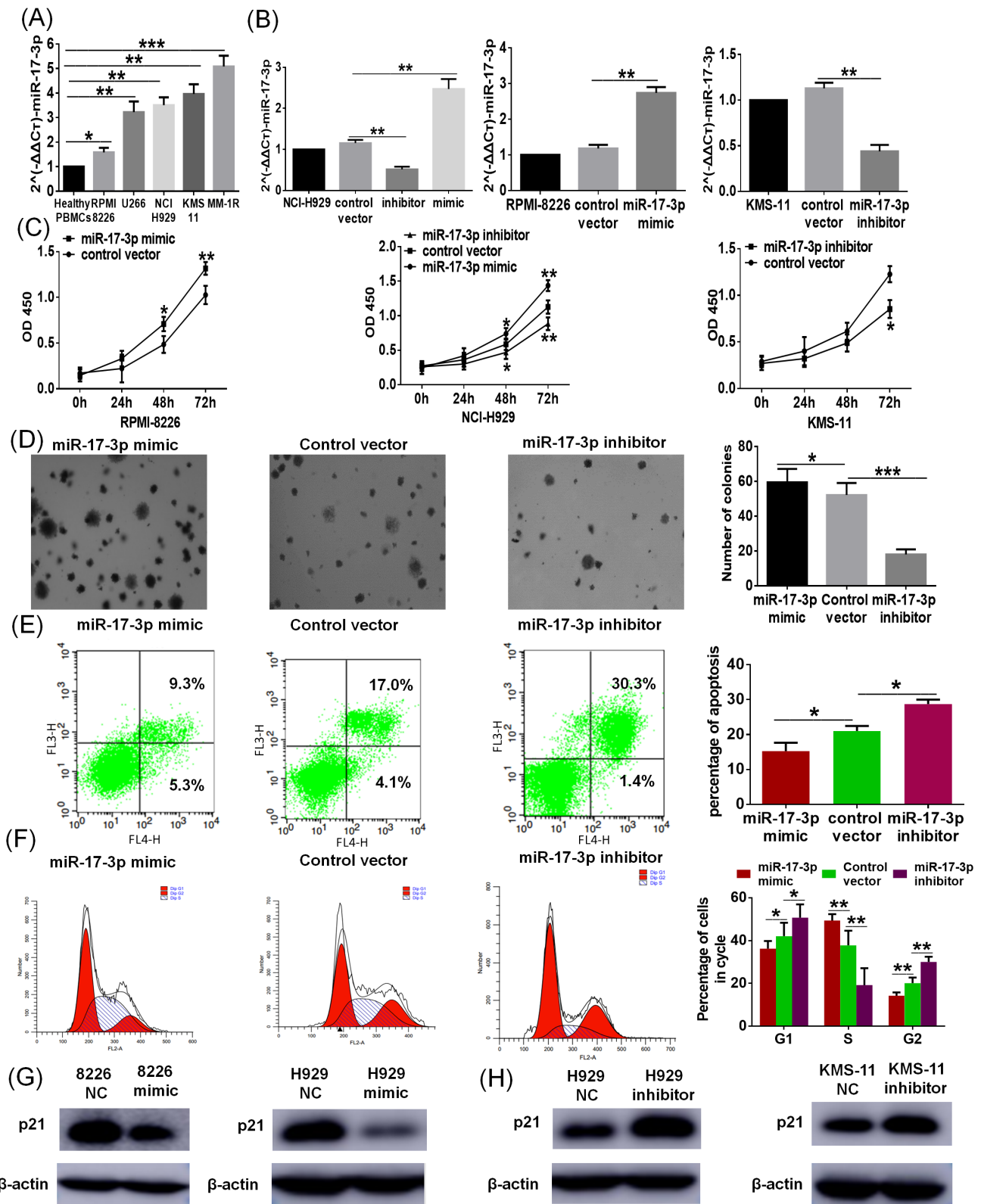


FIGURE 3 miR-17-3p is upregulated in multiple myeloma (MM) cell lines, promotes cell proliferation and colony formation and inhibits MM cell apoptosis and affects the cell cycle. A, Expression levels of miR-17-3p in five MM cell lines and healthy PBMCs. B, miR-17-3p expression levels in RPMI-8226 cells, NCI-H929 cells and KMS-11 cells transfected with negative control (NC) or miR-17-3p mimics or inhibitors. C, CCK-8 assays were performed to assess cell proliferation, which was detected 0, 24, 48 and 72 hours after miR-17-3p mimic or inhibitor transfection. D, Soft agar assays were performed to assess the colony formation of MM cells transfected with miR-17-3p mimics or inhibitors (* $P < .05$; ** $P < .01$; *** $P < .001$). E, F, Flow cytometry was used to assess cell apoptosis (E) and the cell cycle (F) after miR-17-3p mimic or inhibitor transfection (* $P < .05$; ** $P < .01$). G, H, Western blotting (WB) was used to measure the protein level of P21 in MM cells transfected with miR-17-3p mimics or inhibitors [Color figure can be viewed at wileyonlinelibrary.com]

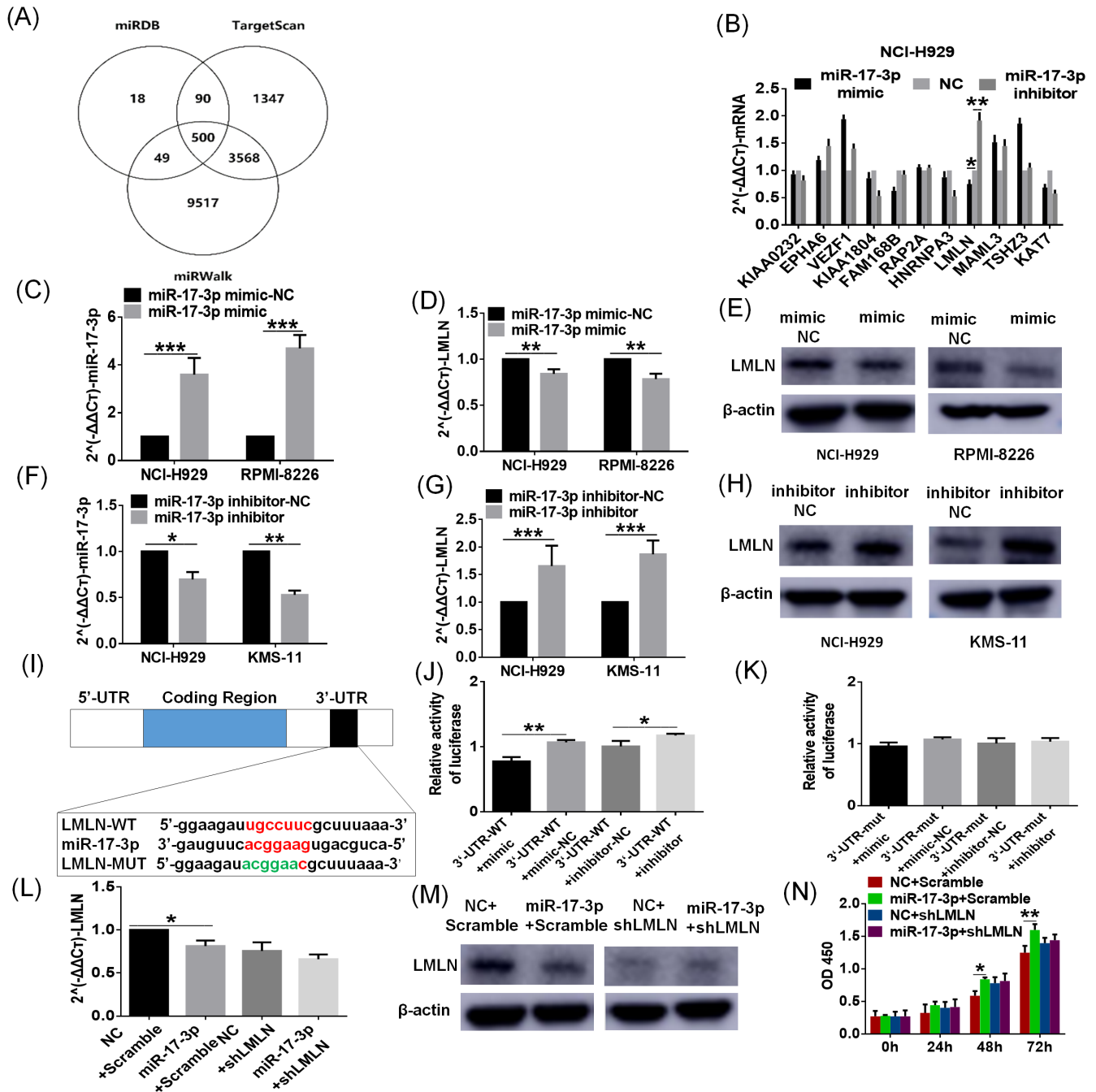


FIGURE 4 LMLN is a direct target of miR-17-3p. A, Prediction of the target gene of miR-17-3p using miRDB, TargetScan and miRWalk software. B, LMLN was identified as a potential target gene of miR-17-3p via RT-PCR. C-H, The expression of LMLN at the mRNA (D,G) and protein levels (E,H) in MM cells transfected with NC, miR-17-3p mimic or miR-17-3p inhibitor (C,F) (* $P < .05$, ** $P < .01$). I, The wild-type and mutated binding sites of the LMLN 3'-UTR region and the miR-17-3p sequence. J,K, Dual-luciferase reporter assay. HEK-293 T cells were cotransfected with luciferase reporter constructs containing wild-type (WT) or mutated LMLN 3'-UTR (MUT) and NC or miR-17-3p mimic or inhibitor. L-N, Rescue experiments confirmed that LMLN was the functional target of miR-17-3p. Expression of LMLN in MM cells at the mRNA level (L) and protein level (M) after transfection with NC and miR-17-3p mimic or shLMLN. N, CCK-8 assay was used to measure MM cell proliferation rates. The OD 450 was detected at 0, 24, 48 and 72 hours (* $P < .05$; ** $P < .01$; *** $P < .001$) [Color figure can be viewed at wileyonlinelibrary.com]

NCI-H929 and KMS-11 cells with miR-17-3p inhibitors. The results showed that miR-17-3p overexpression decreased the mRNA level of LMLN, while miR-17-3p inhibition increased the mRNA level of LMLN (Figure 4C,D,F,G) as well as the protein level (Figure 4E,H) compared to those in the control group. To determine whether LMLN is a target

gene of miR-17-3p, we used a dual-luciferase reporter gene assay for validation. The predicted sequence of the binding site of miR-17-3p and the LMLN 3'-UTR region and the sequence after mutation are shown in Figure 4I. We incorporated 400 bp, including the binding site sequence, into the pmirGLO vector to construct a recombinant

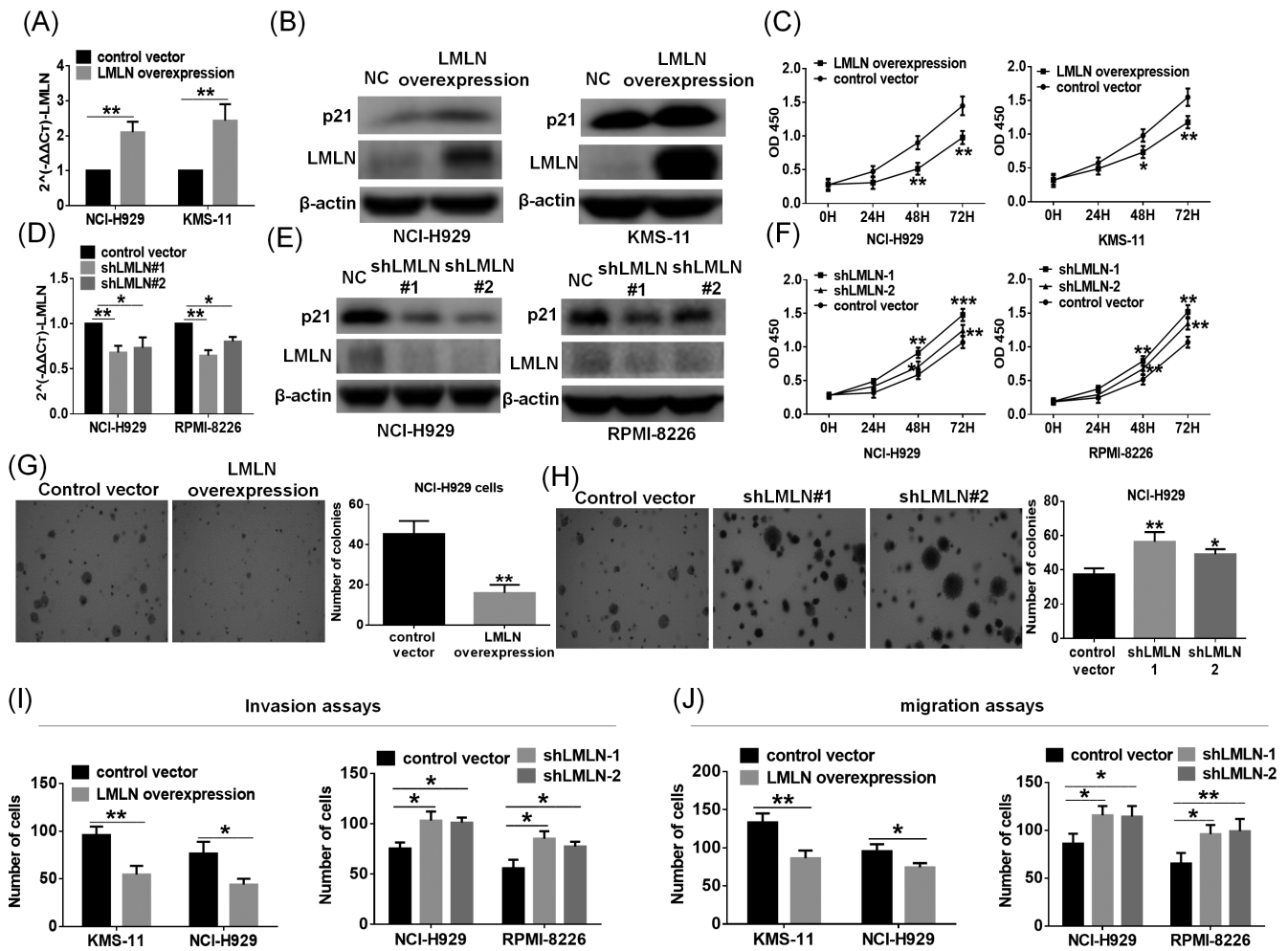


FIGURE 5 LMLN inhibited multiple myeloma (MM) cell proliferation and colony formation by downregulating P21 expression. Expression at the mRNA and protein levels was evaluated by RT-PCR and western blot analyses after transduction of NCI-H929 or KMS-11 cells with control lentivirus or LMLN overexpression lentivirus (A,B) and transduction of NCI-H929 and RPMI-8226 cells with control lentivirus or shLMLN lentivirus (D,E). C,F, CCK-8 assay was used to measure MM cell proliferation rates. The OD 450 was detected at 0, 24, 48 and 72 hours. G,H, Colony formation was monitored after LMLN overexpression or knockdown in the NCI-H929 cell line. I,J, Invasion and migration assays were monitored after LMLN overexpression (NCI-H929 and KMS-11 cell lines) or knockdown (NCI-H929 and RPMI-8226 cell lines) in the MM cell lines. (* $P < .05$; ** $P < .01$ and *** $P < .001$)

plasmid. The miR-17-3p mimics, NC, miR-17-3p inhibitor and the recombinant plasmid were cotransfected into HEK 293T cells and incubated for 48 hours to check the fluorescence intensity. The results showed that the fluorescence value of the miR-17-3p mimics and recombinant plasmid cotransfection group was lower than that of the miR-17-3p inhibitor and recombinant plasmid cotransfection group (Figure 4J; * $P < .05$; ** $P < .01$). This finding showed that LMLN binds directly with miR-17-3p and is negatively regulated by miR-17-3p. Then, we repeated the above experiment after mutation of the binding site, and the result showed no significant difference in fluorescence values between the groups (Figure 4K). These results suggested that miR-17-3p can directly bind with the 3'-UTR region of LMLN.

A rescue experiment was used to assess whether LMLN is a functional target for miR-17-3p in the NCI-H929 cell line. First, we overexpressed miR-17-3p in control scramble cells or LMLN knockdown cells and detected the mRNA and protein levels of LMLN. The results showed that overexpression of miR-17-3p could decrease the mRNA

and protein levels of LMLN (Figure 4L,M). Then, we used the CCK-8 assay to check whether LMLN depletion can influence miR-17-3p's effect on cell proliferation. The results showed that overexpression of miR-17-3p promoted NCI-H929 cell proliferation; however, when LMLN was depleted, the proproliferative effect of miR-17-3p was diminished (Figure 4N). The results suggest that LMLN is a functional downstream target of miR-17-3p.

4.5 | LMLN acts as a tumor suppressor gene in MM cells

We previously found that LMLN is the target gene of miR-17-3p and that miR-17-3p negatively regulates P21. Next, we studied the effect of LMLN on the proliferation of MM cells and whether there is some interaction between LMLN and P21. We overexpressed LMLN in NCI-H929 and KMS-11 cell lines and checked the mRNA and protein

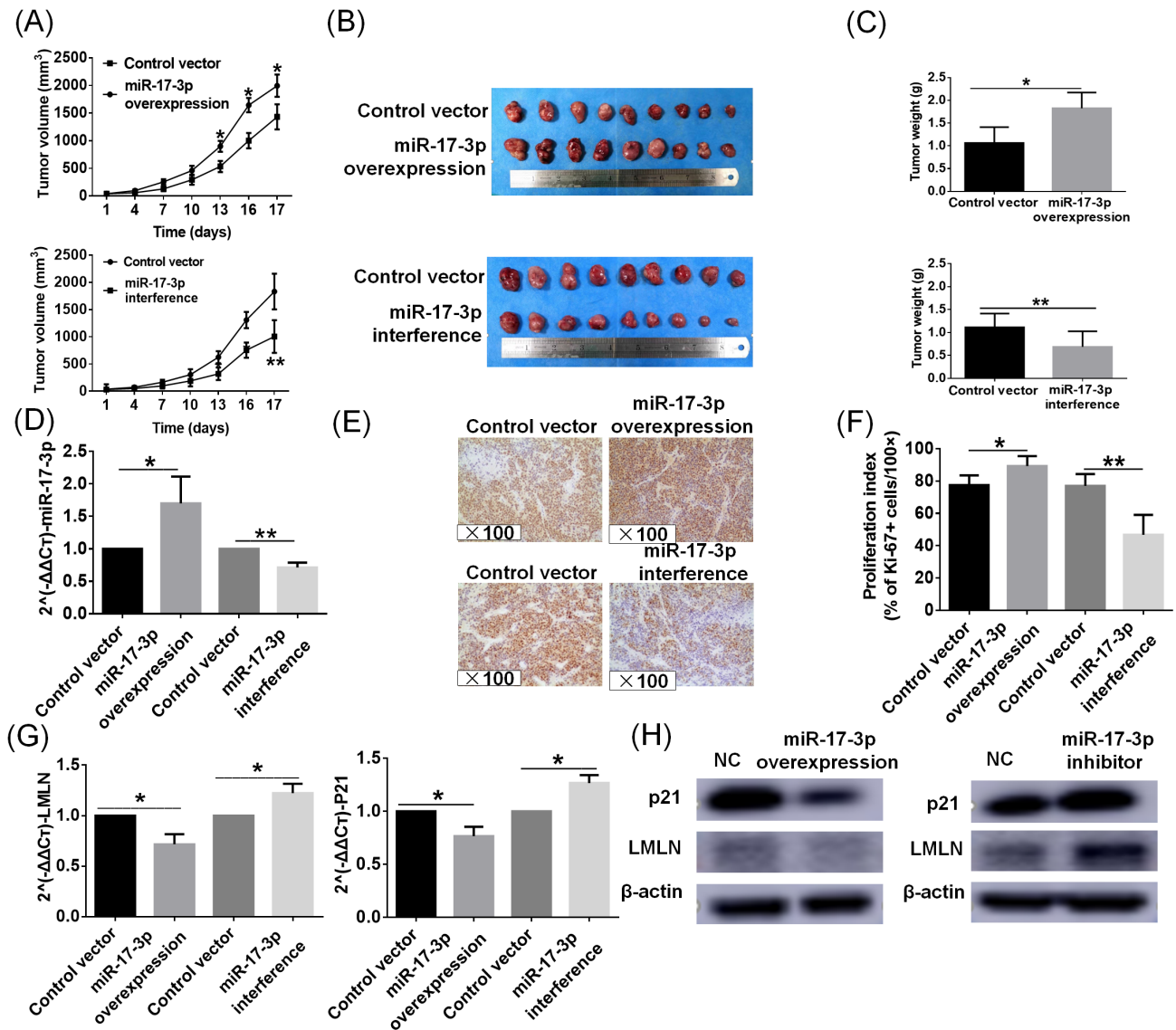


FIGURE 6 miR-17-3p promotes tumorigenicity in vivo. A, The volumes of tumors from mice xenografted with control lentivirus, miR-17-3p mimics lentivirus or miR-17-3p inhibitor lentivirus. B, Images of xenograft tumors from mice subcutaneously injected with control lentivirus, miR-17-3p mimics lentivirus or miR-17-3p inhibitor lentivirus. C, Tumor weights were compared between the control lentivirus, miR-17-3p mimics lentivirus and miR-17-3p inhibitor lentivirus groups. D, Expression levels of miR-17-3p in xenograft tumors were measured by RT-PCR. E, F, Immunohistochemical staining of Ki-67 in tumor tissues dissected from nude mice transfected with miR-17-3p mimics or inhibitor lentivirus. G, H, Expression levels of LMLN and P21 in xenograft tumors were measured by RT-PCR (G) and WB (H) (* $P < .05$; ** $P < .01$) [Color figure can be viewed at wileyonlinelibrary.com]

levels of LMLN and P21 by qPCR and WB (Figure 5A, B). The results of the CCK-8 assay showed that LMLN inhibited the proliferation of MM cells (Figure 5C). In contrast, after knockdown of LMLN expression at the mRNA and protein levels (Figure 5D, E), CCK-8 assays showed that cell proliferation was accelerated (Figure 5F). The results of the soft agar assay showed that LMLN overexpression inhibited MM cell colony formation compared to that in the control group (Figure 5G, H). According to NCBI, we know that LMLN could affect cells invasion and migration, we further explored the effect of LMLN overexpression or knockdown on MM cells invasion and migration. The results showed that overexpression of LMLN reduced the invasion and migration of MM cells (Figure 5I). On the contrary, knockdown of LMLN enhanced the

invasion and migration of MM cells (Figure 5J). The above results suggested that LMLN acts as a tumor suppressor in MM cell lines. The findings demonstrated that LMLN overexpression exerts an effect opposite to that induced by miR-17-3p.

4.6 | miR-17-3p promotes tumor growth in vivo

We studied the expression level of miR-17-3p in the BM and plasma of MM patients as well as its expression and role in MM cell lines. We then studied the effect of miR-17-3p on the tumorigenesis of subcutaneous xenografts in nude mice. Compared to the control group, the

miR-17-3p overexpression group had a larger tumor volume and heavier tumor weight. In contrast, the tumor volume of the miR-17-3p knockdown group was smaller than that of the control group, and the tumor weight was lighter (Figure 6A-C). The expression level of miR-17-3p in the tumors was approximated using RT-PCR (Figure 6D). IHC results of tumor tissues showed that the Ki-67 staining of the miR-17-3p overexpression group was stronger than that of the miR-17-3p inhibitor group (Figure 6E,F). Then, we checked the mRNA and protein levels of LMLN and P21 in the tumor tissues by qPCR and WB (Figure 6G,H). These *in vivo* results were consistent with the results from cytology experiments.

5 | DISCUSSION

MM is a hematological malignancy characterized by abnormal clonal proliferation and expansion of malignant myeloid cells.^{38,39} Although great progress has been made in understanding the pathogenesis of MM and developing potential effective therapies, the disease remains incurable.⁴⁰ Therefore, new diagnostic methods are urgently needed to ensure early detection of MM and to help in the development of new targeted drugs. This will improve prognosis and extend the overall survival of patients. miRNAs are endogenous short noncoding single-stranded regulatory RNA molecules with a length of 18 to 25 nucleotides. They regulate the expression of target genes at the post-transcriptional level by binding to the 3'-UTR region of specific messenger RNA (mRNA).^{41,42} In recent years, studies have shown that miRNA expression is abnormal in many cancers, including MM. It has been further demonstrated that miRNA can be used as a tumor indicator to regulate cell proliferation, migration, cycle and differentiation.^{43,44} For example, the expression of miR-15a, miR-16-1 and miR-17-92 has been implicated in the poor prognosis of MM.⁴⁵ In another study, Wu Ping et al found that miR-17 was closely related to the overall survival of MM patients.⁴⁶ In our study, a miRNA 4.0 microarray was used to detect the miRNA expression profiles of the BM of NDMM patients and healthy subjects. We found that the top 10 miRNAs, including miR-17-3p, with the most significant expression differences were all highly expressed in NDMM. However, the specific role and mechanism of miR-17-3p in MM has not been elucidated. Based on the results of previous experiments, we considered that miR-17-3p has an important role in MM that needs to be unraveled.

MM is a malignant tumor of the blood system with a poor prognosis. Currently, MM diagnosis is mainly based on BM aspiration, biopsy and hematology index. The first two operations are invasive, and because plasma cells are clustered in the BM, the repeatability of the operation is poor. In addition, it remains difficult to accurately diagnose MM patients during the early stages of the disease due to the lack of simple and effective molecular biomarkers. miRNAs exist in cells as well as various other body fluids, including serum and plasma.⁴⁷ In our study, we expanded the sample size to detect the expression of miR-17-3p in the BM and plasma of MM patients as well as healthy subjects. We found that the expression trend of miR-17-3p in the BM and plasma of MM was consistent. The results showed that miR-17-3p levels in the NDMM

and RRMM patients were higher than those in the healthy subjects ($P < .05$). The expression levels of miR-17-3p in the CRMM and MGUS patients were slightly higher than those in the healthy subjects, although the differences were not statistically significant. In addition, the expression of miR-17-3p was positively correlated with the ISS stage. We then analyzed the relationship between plasma miR-17-3p expression and BMPC abundance and serum M protein level in NDMM patients. The relative expression levels of miR-17-3p in plasma were positively correlated with the abundance of BMPCs ($P < .01$, $r = 0.6249$) and the abnormal expression of serum M protein ($P < .05$, $r = 0.4294$), suggesting that plasma miR-17-3p might be a diagnostic biomarker for MM. The results of the ROC curve analysis showed that plasma miR-17-3p has high accuracy and specificity as a diagnostic biomarker of MM.

We further studied the expression level of miR-17-3p in MM cell lines and evaluated its biological effects *in vitro* and *in vivo*. We observed a higher expression level of miR-17-3p in MM cell lines than in normal human BM mononuclear cells. Functionally, miR-17-3p can promote the proliferation and colony formation of MM cells, inhibit apoptosis and regulate the cell cycle. To clarify the mechanism by which miR-17-3p affects the cell cycle of MM cells, we identified the related CDK inhibitor by WB. The results showed that the expression of P21 protein was negatively correlated with the expression of miR-17-3p. Therefore, we believe that miR-17-3p can affect the expression of P21 and then affect the cell cycle and proliferation.

We also predicted target genes of miR-17-3p using software and verified their expression via RT-PCR. We found that miR-17-3p can negatively regulate LMLN expression at both the mRNA and protein levels. Consequently, we concluded that LMLN may be a target gene of miR-17-3p. Recent studies have demonstrated that most miRNAs bind with the 3'-UTR region in the target gene,^{48,49} and we performed dual-luciferase vector reporter experiments to verify whether LMLN is the target gene of miR-17-3p. Our results suggested that miR-17-3p can directly bind to the 3'-UTR region of LMLN. According to NCBI, we know that LMLN is a leishmanolysin-like peptidase and could encode a zinc-metallopeptidase, which may play a role in cell migration, invasion and mitotic progression. P21 is a CDK inhibitor and a tumor suppressor gene that plays an important role in cell growth, differentiation and apoptosis. We found that miR-17-3p could negatively regulate LMLN and P21 and that P21 was positively correlated with LMLN, which suggests that the miR-17-3p-LMLN-P21 axis could regulate MM cell proliferation. At present, there are some studies on LMLN in *Leishmania* and animals, but few researches are present in human tumors.⁵⁰⁻⁵³ In our research, LMLN inhibited the proliferation and colony formation of MM cells and acted as a tumor suppressor, whose effects were opposite to those of miR-17-3p. In future studies, we will focus on the interaction mechanism between LMLN and P21, assess the mechanism of LMLN affects the invasion and migration of MM cells.

6 | CONCLUSION

In summary, miR-17-3p is highly expressed in the plasma and BM cells of MM patients and MM cell lines. The expression of miR-17-3p is

positively correlated with diagnostic indexes such as marrow plasma cell abundance and serum M protein level and is positively correlated with the ISS stage of the disease. It exerts an oncogenic role in MM cells by regulating the proliferation, apoptosis, cell cycle and colony formation of MM cells by targeting LMLN and regulating P21. miR-17-3p could act as a promising diagnostic biomarker for MM in the clinic, and the miR-17-3p-LMLN-P21 axis could be a new target in MM progression.

ACKNOWLEDGMENTS

This work was supported by a grant from the National Natural Science Foundation of China (NSFC) funded by the Chinese government (52110013 to Baijun Fang) and a grant from the Henan Innovation Talent Program funded by Henan Province, China (184200510007 to Baijun Fang).

CONFLICT OF INTEREST

The authors declared no potential conflicts of interest.

DATA AVAILABILITY STATEMENT

The miRNA microarray data generated in this study is available in GEO under accession number: GSE157324. Other data are available from the corresponding authors upon request.

ETHICS STATEMENT

All patients and healthy subjects recruited in the study provided written informed consent. The study protocol conformed to the ethical guidelines of the Helsinki Declaration and was approved by the Scientific Ethics Committee of Henan Cancer Hospital. All procedures involving animals in our study were approved by the Research Ethics Committee of Henan Cancer Hospital.

ORCID

Kangdong Liu  <https://orcid.org/0000-0001-9290-4987>

Baijun Fang  <https://orcid.org/0000-0001-7038-2065>

REFERENCES

- Bianchi G, Anderson KC. Understanding biology to tackle the disease: multiple myeloma from bench to bedside, and back. *CA Cancer J Clin*. 2014;64(6):422-444.
- Allart-Vorelli P, Porro B, Baguet F, Michel A, Cousson-Gélie F. Haematological cancer and quality of life: a systematic literature review. *Blood Cancer J*. 2015;5(4):e305.
- Nathwani N, Larsen JT, Kapoor P. Consolidation and maintenance therapies for newly diagnosed multiple myeloma in the Era of novel agents. *Curt Hematol Malig Rep*. 2016;11(2):127-136.
- Barlogie B, Attal M, Crowley J, et al. Long-term follow-up of auto-transplantation trials for multiple myeloma: update of protocols conducted by the Intergroupe Francophone du Myelome, Southwest Oncologygroup, and University of Arkansas for Medical Sciences. *J Clin Oncol*. 2010;28(7):1209-1214.
- Lokhorst HM, van der Holt B, Zweegman S, et al. A randomized phase3 study on the effect of thalidomide combined with adriamycin, dexamethasone, and high-dose melphalan, followed by thalidomide maintenance in patients with multiple myeloma. *Blood*. 2010;115(6):1113-1120.
- Wu P, Agnelli L, Walker BA, et al. Improved risk stratification in myeloma using a microRNA-based classifier. *Br J Haematol*. 2013;162(3):348-359.
- Ling H, Fabbri M, Calin GA. MicroRNAs and other non-coding RNAs as targets for anticancer drug development. *Nat Rev Drug Discov*. 2013;12(11):847-865.
- Huang X, Lu J. Guidelines for the diagnosis and treatment of multiple myeloma in China (2015 revision). *Chin J Int Med*. 2015;54(12):1066-1070.
- Ambros V. MicroRNAs and developmental timing. *Curr Opin Genet Dev*. 2011;21(4):511-517.
- Ambros V, Chen X. The regulation of genes and genomes by small RNAs. *Dev Camb Engl*. 2007;134(9):1635-1641.
- Ambros V. The functions of animal microRNAs. *Nature*. 2004;431(7006):350-355.
- Bartel DP. Metazoan MicroRNAs. *Cell*. 2018;173(1):20-51.
- Bartel DP. MicroRNAs: genomics, biogenesis, mechanism, and function. *Cell*. 2004;116(34):281-297.
- Li F, Xu Y, Deng S, et al. MicroRNA-15a/16-1 cluster located at chromosome 13q14 is down-regulated but displays different expression pattern and prognostic significance in multiple myeloma. *Oncotarget*. 2015;6(35):38270-38282.
- Khoshnevisan A, Parvin M, Ghorbanmehr N, et al. A significant upregulation of miR5-886-p in high grade and invasive bladder tumors. *Urol J*. 2015;12(3):2160-2164.
- Li JH, Xiao X, Zhang YN, et al. MicroRNA MIR-886-5P inhibits apoptosis by down-regulating Bax expression in human cervical carcinoma cells. *Gynecol Oncol*. 2011;120(1):145-151.
- Zhang LL, Wu J, Liu Q, Zhang Y, Sun ZL, Jing H. miR-886-5p inhibition inhibits growth and induces apoptosis of MCF7 cells. *Asian Pac J Cancer Prev*. 2014;15(4):1511-1515.
- Wu P, Agnelli L, Walker BA, et al. Improved risk stratification in myeloma using a microRNA-based classifier. *Br J Haematol*. 2013;162(3):348-359.
- Chng WJ, Dispenzieri A, Chim CS, et al. IMWG consensus on risk stratification in multiple myeloma. *Leukemia*. 2014;28(2):269-277.
- Sun CY, She XM, Qin Y, et al. miR-15a and miR-16 affect the angiogenesis of multiple myeloma by targeting VEGF. *Carcinogenesis*. 2013;34(2):426-435.
- Misiewicz-Krzeminska I, Sarasquete ME, Quwaider D, et al. Restoration of microRNA-214 expression reduces growth of myeloma cells through positive regulation of P53 and inhibition of DNA replication. *Haematologica*. 2013;98(4):640-648.
- Quwaider D, Corchete LA, Misiewicz KI, et al. DEPTOR maintains plasma cell differentiation and favorably affects prognosis in multiple myeloma. *J Hematol Oncol*. 2017;10(1):92.
- Li Y, Zhang B, Li W, et al. MiR-15a/16 regulates the growth of myeloma cells, angiogenesis and antitumor immunity by inhibiting Bcl-2, VEGF-A and IL-17 expression in multiple myeloma. *Leuk Res*. 2016;49(7):73-79.
- Amodio N, Stamato MA, Gullà AM, et al. Therapeutic targeting of miR-29b/HDAC4 epigenetic loop in multiple myeloma. *Mol Cancer Ther*. 2016;15(6):1364-1375.
- Lu Y, Wu D, Wang J, Li Y, Chai X, Kang Q. miR-320a regulates cell proliferation and apoptosis in multiple myeloma by targeting pre-B-cell leukemia transcription factor 3. *Biochem Biophys Res Commun*. 2016;473(4):1315-1320.
- Yu T, Zhang X, Zhang L, et al. MicroRNA-497 suppresses cell proliferation and induces apoptosis through targeting PBX3 in human multiple myeloma. *Am J Cancer Res*. 2016;6(12):2880-2889.
- Yang Y, Li F, Saha MN, Abdi J, Qiu L, Chang H. miR-137 and miR-197 induce apoptosis and suppress tumorigenicity by targeting MCL-1 in multiple myeloma. *Clin Cancer Res*. 2015;21(10):2399-2411.
- Huang E, Liu R, Chu Y. miRNA-15a/16: as tumor suppressors and more. *Future Oncol*. 2015;11(16):2351-2363.

29. Tung YT, Huang PW, Chou YC, et al. Lung tumorigenesis induced by human vascular endothelial growth factor(hVEGF)-A165 over-expression in transgenic mice and amelioration of tumor formation by miR-16. *Oncotarget*. 2015;6(12):10222-10238.
30. Bian C, Liu T, Liu X. Function of microRNAs in animals. *J Med Mol Biol*. 2005;6(12):10222-10238.
31. Altuvia Y, Landgraf P, Lithwick G, et al. Clustering and conservation patterns of human microRNAs. *Nucleic Acids Res*. 2005;33(8):2697-2706.
32. Ambros V. MicroRNAs and developmental timing. *Curr Opin Genet Dev*. 2011;21(4):511-517.
33. Chen L, Li C, Zhang R, et al. miR-17-92 cluster microRNAs confers tumorigenicity in multiple myeloma. *Cancer Lett*. 2011;309(1):62-70.
34. Gao X, Zhang R, Qu X, et al. MiR-15a, miR-16-1 and miR-17-92 cluster expression are linked to poor prognosis in multiple myeloma. *Leuk Res*. 2012;36(21):1505-1509.
35. Lang T, Nie Y. miR-148a participates in the growth of RPMI8226 multiple myeloma cells by regulating CDKN1B. *Biomed Pharmacother*. 2016;84:1967-1971.
36. Kyle RA, Gertz MA, Witzig TE, et al. Review of 1027 patients with newly diagnosed multiple myeloma. *Mayo Clin Proc*. 2003;78(1):21-33.
37. Cobbe N, Marshall KM, Gururaja Rao S, et al. The conserved metalloprotease invadolysin localizes to the surface of lipid droplets. *J Cell Sci*. 2009;122:3414-3423.
38. Gullà A, Di Martino MT, Gallo Cantafio ME, et al. A 13 mer LNA-miR-221 inhibitor restores drug sensitivity in melphalan-refractory multiple myeloma cells. *Clin Cancer Res*. 2015;22(5):1222.
39. Noll JE, Hewett DR, Williams SA, et al. SAMS1 is a tumor suppressor gene in multiple myeloma. *Neoplasia*. 2014;16(7):572-585.
40. Zhao JJ, Lin J, Zhu D, et al. miR-30-5p functions as a tumor suppressor and novel therapeutic tool by targeting the oncogenic Wnt/-catenin/BCL9 pathway. *Cancer Res*. 2014;74(6):1801-1813.
41. Chen S, Chen X, Xiu YL, Sun KX, Zhao Y. MicroRNA-490-3P targets CDK1 and inhibits ovarian epithelial carcinoma tumorigenesis and progression. *Cancer Lett*. 2015;362(1):122-130.
42. Li C, Nie H, Wang M, et al. MicroRNA-409-3p regulates cell proliferation and apoptosis by targeting PHF10 in gastric cancer. *Cancer Lett*. 2012;320(2):197.
43. Ma J, Yao Y, Wang P, et al. MiR-152 functions as a tumor suppressor in glioblastoma stem cells by targeting Krüppel-like factor 4. *Cancer Lett*. 2014;355(1):85-95.
44. Zhao Z, Ma X, Sung D, et al. microRNA-449a functions as a tumor suppressor in neuroblastoma through inducing cell differentiation and cell cycle arrest. *RNA Biol*. 2015;12(5):538-554.
45. Gao X, Zhang R, Qu X, et al. miR-15a, miR-16-1 and miR-17-92 cluster expression are linked to poor prognosis in multiple myeloma. *Leuk Res*. 2012;36(12):1505-1509.
46. Wu P, Agnelli L, Walker BA, et al. Improved risk stratification in myeloma using a microRNA-based classifier. *Br J Haematol*. 2013;162(3):348-359.
47. Turchinovich A, Samatov TR, Tonevitsky AG, et al. Circulating miRNAs: cell-cell communication function? *Front Genet*. 2013;4(10):119.
48. Lewis BP, Burge CB, Bartel DP. Conserved seed pairing, often flanked by adenosines, indicates that thousands of human genes are microRNA targets. *Cell*. 2005;120(1):15-20.
49. Rajewsky N. microRNA target predictions in animals. *Nat Genet*. 2006;38(6):10-15.
50. Rampoldi A, Jacobsen MJ, Bertschinger HU, et al. The receptor locus for *Escherichia coli* F4ab/F4ac in the pig maps distal to the MUC4-LMLN region. *Mamm Genome*. 2011;22(1-2):122-129.
51. Vass S, Heck MM. Perturbation of invadolysin disrupts cell migration in zebrafish (*Danio rerio*). *Exp Cell Res*. 2013;319(8):1198-1212.
52. Gimenez-Xavier P, Pros E, Bonastre E, et al. Genomic and molecular screenings identify different mechanisms for acquired resistance to MET inhibitors in lung cancer cells. *Mol Cancer Ther*. 2017;7(16):7.
53. Xu Z, Sun H, Zhang Z, et al. Assessment of autozygosity derived from runs of homozygosity in Jinhua pigs disclosed by sequencing data. *Front Genet*. 2019;10:274.

SUPPORTING INFORMATION

Additional supporting information may be found online in the Supporting Information section at the end of this article.

How to cite this article: Xiang P, Yeung YT, Wang J, et al. miR-17-3p promotes the proliferation of multiple myeloma cells by downregulating P21 expression through LMLN inhibition. *Int. J. Cancer*. 2021;148:3071–3085. <https://doi.org/10.1002/ijc.33528>